Eur. Phys. J. B **58**, 297–309 (2007)
DOI: 10.1140/epjb/e2007-00223-3

THE EUROPEAN PHYSICAL JOURNAL B

Non-perturbative renormalization group calculation of the scalar self-energy

J.-P. Blaizot[1,a], R. Méndez-Galain[2], and N. Wschebor[2]

[1] ECT*, Villa Tambosi, strada delle Tabarelle 286, 38050 Villazzano (TN), Italy
[2] Instituto de Física, Facultad de Ingeniería, J.H.y Reissig 565, 11000 Montevideo, Uruguay

Received 31 July 2006 / Received in final form 19 June 2007
Published online 8 September 2007 –

Abstract. We present the first numerical application of a method that we have recently proposed to solve the Non Perturbative Renormalization Group equations and obtain the n-point functions for arbitrary external momenta. This method leads to flow equations for the n-point functions which are also differential equations with respect to a constant background field. This makes them, a priori, difficult to solve. However, we demonstrate in this paper that, within a simple approximation which turns out to be quite accurate, the solution of these flow equations is not more complicated than that of the flow equations obtained in the derivative expansion. Thus, with a numerical effort comparable to that involved in the derivative expansion, we can get the full momentum dependence of the n-point functions. The method is applied, in its leading order, to the calculation of the self-energy in a 3-dimensional scalar field theory, at criticality. Accurate results are obtained over the entire range of momenta.

PACS. 05.10.Cc Renormalization group methods – 11.15.Tk Other nonperturbative techniques

1 Introduction

The non perturbative renormalization group (NPRG) [1–5] stands out as a very promising formalism to address non perturbative problems, i.e., problems in which the absence of a small parameter prevents one to build a solution in terms of a systematic expansion. It leads to exact flow equations which are difficult to solve in general, but which offer the possibility for new approximation schemes. When only correlation functions at small momenta are needed, as is the case for instance in the calculation of critical exponents, a general approximation method to solve the infinite hierarchy of the NPRG equations has been developped [5–7]. This method, which can be systematically improved, is based on a derivative expansion of the effective action. It has been applied successfully to a variety of physical problems, in condensed matter, particle or nuclear physics (for reviews, see e.g. [6, 7]). However, in many situations, this is not enough: in order to calculate the quantities of physical interest, the knowledge of the full momentum dependence of the correlation functions is mandatory. Many efforts to get this information from the flow equations, involve truncations of various kinds [8], following an early suggestion by Weinberg [9] (see however [10, 11]).

The present paper explores the applicability of the strategy that we proposed recently in [14], following our previous works [19, 20] in which we presented a scheme to obtain the momentum dependence of n-point functions from the flow equations. The strategy put forward in [14] is based on the fact that the internal momentum q in the integrals that determine the flow of the n-point functions is bounded by the regulator introduced by the NPRG. Since this regulator also guarantees that the vertex functions are smooth functions of the momenta, these can be expanded in powers of q^2/κ^2, κ being the cut-off scale in the regulator. The "leading order" (LO) of the approximation scheme proposed in [14] simply consists in keeping the lowest order of this expansion, i.e., in setting $q = 0$ in the vertices. Doing so, and working in a constant external field, it is possible to relate to each other the various n-point functions that appear in a given flow equation through derivatives with respect to the external field, thereby closing the hierarchy of equations.

In [14] we showed that the method reproduces perturbative results, at any desired order. Furthermore, we also showed that the LO is exact in the large N limit of the $O(N)$ scalar model. Finally, one expects the method to provide results as good as those of the derivative expansion at small momenta. It is beyond the scope of the present paper to address the general issue of the convergence of our approximation scheme. The convergence of the derivative expansion remains, to a large extent, an open problem which has been addressed, for instance, in [15] or, more recently, in [18]. The quality of the derivative expansion

[a] e-mail: blaizot@spht.saclay.cea.fr

can however be gauged from numerous applications in various contexts (see e.g. [12, 16, 17, 24], and also [6, 7]). Its convergence seems to be better when the anomalous dimension is small, which is the case for the scalar model studied in this paper.

The price to pay for relating the n-point functions in the flow equations through derivatives with respect to a uniform background field is that the flow equations become differential equations with respect to this uniform background field, with integral kernels that involve the solution itself. These integro-differential equations are a priori difficult to solve. The aim of this paper is to demonstrate that they can indeed be solved, with a numerical effort comparable to that involved in solving the flow equations that result from the derivative expansion, and to present a first application to the study of the 2-point correlation function of the scalar model, in the LO of the approximation scheme.

The outline of the paper is as follows. In Section 2 we briefly recall some basic features of the NPRG and the essence of our approximation scheme in the case of a scalar field theory. In Section 3 we analyze the structure of the flow equation for the 2-point correlation function and describe the strategy that we used to solve it. In Section 4 we present numerical results for the self-energy of the scalar field, at criticality and in $d = 3$. The appendices gather technical material.

2 The method

We consider a scalar field theory with the classical action

$$S = \int \mathrm{d}^d x \left\{ \frac{1}{2} \left(\partial_\mu \varphi(x)\right)^2 + \frac{r}{2}\,\varphi^2(x) + \frac{u}{4!}\,\varphi^4(x) \right\}. \quad (1)$$

The NPRG constructs a family of effective actions, $\Gamma_\kappa[\phi]$ (with ϕ the expectation value of the field in the presence of external sources), in which the magnitude of long wavelength fluctuations are controlled by an infrared regulator depending on a continuous parameter κ. The effective action $\Gamma_\kappa[\phi]$ interpolates between the classical action obtained for $\kappa = \Lambda$ (with Λ the microscopic scale at which fluctuations are essentially suppressed), and the full effective action obtained when $\kappa \to 0$, i.e., when all fluctuations are taken into account (see e.g. [7]). It is understood that the values of the parameters r and u of the classical action (1), as well as the field normalisation, are fixed at the microscopic scale Λ. One can write for $\Gamma_\kappa[\phi]$ an exact flow equation [3–5]:

$$\partial_\kappa \Gamma_\kappa[\phi] = \frac{1}{2} \int \frac{d^d q}{(2\pi)^d} (\partial_\kappa R_\kappa(q)) \left[\Gamma_\kappa^{(2)} + R_\kappa \right]^{-1}_{q,-q}, \quad (2)$$

where $\Gamma_\kappa^{(2)}$ is the second derivative of Γ_κ with respect to ϕ, and R_κ denotes a family of "cut-off functions" depending on κ. There is a large freedom in the choice of $R_\kappa(q)$, abundantly discussed in the literature [21–24]. To be specific, in the present paper, we shall use for $R_\kappa(q)$ the following function [23]

$$R_\kappa(q) = Z_\kappa(\kappa^2 - q^2)\,\Theta(\kappa^2 - q^2), \quad (3)$$

where Z_κ is a function of κ specified in the next section (see Eq. (18)).

By deriving equation (2) with respect to ϕ, and then letting the field be constant, one gets the flow equation for the n-point functions $\Gamma^{(n)}$ in a constant background field ϕ. More precisely, taking into account momentum conservation, one defines:

$$(2\pi)^d\,\delta^{(d)}(p_1 + \cdots + p_n)\;\Gamma_\kappa^{(n)}(p_1, \ldots, p_n; \phi) = \int d^d x_1 \ldots \int d^d x_n e^{i\sum_{j=1}^n p_j x_j}\; \frac{\delta^n \Gamma_\kappa}{\delta\phi(x_1)\ldots\delta\phi(x_n)}\bigg|_{\phi(x)\equiv\phi}. \quad (4)$$

Then, the equation for the 2-point function reads:

$$\partial_\kappa \Gamma_\kappa^{(2)}(p;\phi) = \int \frac{d^d q}{(2\pi)^d} (\partial_\kappa R_\kappa(q)) \Big\{ G_\kappa(q;\phi)\Gamma_\kappa^{(3)}(p, q, -p-q;\phi) \times G_\kappa(q+p;\phi)\Gamma_\kappa^{(3)}(-p, p+q, -q;\phi)G_\kappa(q;\phi) - \frac{1}{2}\, G_\kappa(q;\phi)\Gamma_\kappa^{(4)}(p, -p, q, -q;\phi)G_\kappa(q;\phi) \Big\}, \quad (5)$$

where

$$G_\kappa^{-1}(q;\phi) \equiv \Gamma_\kappa^{(2)}(q;\phi) + R_\kappa(q), \quad (6)$$

and in equations (5) and (6) we have used the simplified notation $\Gamma_\kappa^{(2)}(q;\phi)$ for $\Gamma_\kappa^{(2)}(q, -q;\phi)$, a notation that will be used throughout.

In general, the flow equation for a given n-point function involves the m-point functions with $m = n + 1$ and $m = n + 2$. Thus, the flow equations for the n-point functions do not close, but constitute an infinite hierarchy of coupled equations; this makes them difficult to solve.

In [14] we proposed a method to solve this infinite hierarchy. It exploits the smoothness of the regularized n-point functions at small momenta, and the fact that the loop momentum q in the right hand side of the flow equations (such as Eq. (2) or Eq. (5)) is limited to $q \lesssim \kappa$ by the presence of the regulator $R_\kappa(q)$. The leading order (LO) of the method presented in [14] thus consists in setting $q = 0$ in the n-point functions in the r.h.s. of the flow equations, for instance

$$\Gamma_\kappa^{(n)}(p_1, p_2, ..., p_{n-1}+q, p_n-q) \sim \Gamma_\kappa^{(n)}(p_1, p_2, ..., p_{n-1}, p_n). \quad (7)$$

Once this approximation is made, some momenta in some of the n-point functions vanish, and the corresponding n-point functions can be obtained as the derivatives of m-point functions ($m < n$) with respect to a constant background field, thereby allowing us to close the hierarchy of equations.

Specifically, in equation (5) for the 2-point function, the 3- and 4-point functions in the r.h.s. will contain respectively one and two vanishing momenta after we set

$q = 0$. These can be related to the following derivatives of the 2-point function:

$$\Gamma_\kappa^{(3)}(p,-p,0;\phi) = \frac{\partial \Gamma_\kappa^{(2)}(p;\phi)}{\partial\phi},$$
$$\Gamma_\kappa^{(4)}(p,-p,0,0;\phi) = \frac{\partial^2 \Gamma_\kappa^{(2)}(p;\phi)}{\partial\phi^2}. \quad (8)$$

One then arrives at a closed equation for $\Gamma_\kappa^{(2)}(p;\rho)$ (with $\rho \equiv \phi^2/2$):

$$\kappa\partial_\kappa \Gamma_\kappa^{(2)}(p;\rho) = J_d^{(3)}(p;\kappa;\rho) \left(\frac{\partial \Gamma_\kappa^{(2)}(p;\rho)}{\partial\phi}\right)^2 - \frac{1}{2} I_d^{(2)}(\kappa;\rho) \frac{\partial^2 \Gamma_\kappa^{(2)}(p;\rho)}{\partial\phi^2}, \quad (9)$$

where

$$J_d^{(n)}(p;\kappa;\rho) \equiv \int \frac{d^dq}{(2\pi)^d} \kappa(\partial_\kappa R_\kappa(q)) G_\kappa(p+q;\rho) G_\kappa^{(n-1)}(q;\rho), \quad (10)$$

and

$$I_d^{(n)}(\kappa;\rho) \equiv \int \frac{d^dq}{(2\pi)^d} \kappa(\partial_\kappa R_\kappa(q)) G_\kappa^n(q;\rho) = J_d^{(n)}(p=0;\kappa;\rho). \quad (11)$$

At this point we note that the n-point functions at zero external momenta can all be considered as derivatives of a single function, the effective potential $V_\kappa(\rho)$. For instance,

$$\Gamma_\kappa^{(2)}(p=0;\rho) = \frac{\partial^2 V_\kappa}{\partial\phi^2}. \quad (12)$$

The effective potential satisfies a flow equation which can be deduced from that for the effective action, equation (2), when restricted to constant fields. It reads

$$\kappa\partial_\kappa V_\kappa(\rho) = \frac{1}{2} \int \frac{d^dq}{(2\pi)^d} \kappa(\partial_\kappa R_\kappa(q)) G_\kappa(q;\rho). \quad (13)$$

The second derivative of this equation with respect to the background field yields a flow equation for $\Gamma_\kappa^{(2)}(p=0;\rho)$. Now, this equation does not coincide with equation (9) in which we set $p = 0$: indeed, in contrast to equation (9), the vertices in the equation deduced from equation (13) keep their q-dependence (q being the loop momentum in Eq. (13)). There is therefore an apparent inconsistency in our approximation scheme, that is however easily resolved by treating separately the zero momentum ($p = 0$) and the non-zero momentum ($p \neq 0$) sectors. In fact, in doing so, we get more accuracy in the sector $p = 0$ than in the sector $p \neq 0$.

Let us then write:

$$\Gamma_\kappa^{(2)}(p;\rho) = p^2 + \frac{\partial^2 V_\kappa}{\partial\phi^2} + \Sigma_\kappa(p;\rho), \quad (14)$$

where

$$\Sigma_\kappa(p;\rho) \equiv \Gamma_\kappa^{(2)}(p;\rho) - p^2 - \Gamma_\kappa^{(2)}(p=0;\rho). \quad (15)$$

We shall refer to $\Sigma_\kappa(p;\rho)$ as the self-energy (although it differs from the usual self-energy by the subtraction of the momentum independent contribution $\Gamma_\kappa^{(2)}(p=0;\rho)$). By definition, $\Sigma_\kappa(p=0;\rho) = 0$, and at criticality, $\Gamma_{\kappa=0}^{(2)}(p=0;\rho) = 0$. We then proceed with separate approximations in the two sectors with $p = 0$ and $p \neq 0$.

In the sector $p \neq 0$, it is $\Sigma_\kappa(p;\rho)$, rather than $\Gamma_\kappa^{(2)}(p;\rho)$ which satisfies the approximate equation (9) (strictly speaking, Eq. (9) to which one subtracts the same equation with $p = 0$):

$$\kappa\partial_\kappa \Sigma(p;\rho) = \left[J_d^{(3)}(p;\kappa;\rho) \left(\frac{\partial \Gamma_\kappa^{(2)}(p;\rho)}{\partial\phi}\right)^2 - \frac{1}{2} I_d^{(2)}(\kappa;\rho) \frac{\partial^2 \Gamma_\kappa^{(2)}(p;\rho)}{\partial\phi^2} \right] - [p \to 0]. \quad (16)$$

Equation (16) is the flow equation for the momentum dependent part of the 2-point function at LO of our approximation scheme. It is a partial differential equation with respect to the two real variables, κ and ρ, with the momentum p playing the role of a parameter. It is to be integrated from $\kappa = \Lambda$, with initial condition $\Sigma_\Lambda(p;\rho) = 0$, to $\kappa = 0$ where it yields the physical self-energy $\Sigma(p;\rho) \equiv \Sigma_{\kappa=0}(p;\rho)$.

Equation (16) is to be solved together with the equation in the sector $p = 0$, i.e., with the equation for the effective potential, with initial condition $V_\Lambda(\rho) = r\rho + (u/6)\rho^2$. In equation (13) for $V_\kappa(\rho)$, we use the propagator (14) in which $\Sigma_\kappa(p;\rho)$ is solution of equation (16) and $\Gamma_\kappa^{(2)}(q=0;\rho)$ is determined self-consistently from the effective potential, using equation (12).

It is not difficult to verify that (in the perturbative regime) this scheme has 2-loop accuracy for the effective potential, and only one-loop accuracy for the self-energy. Besides, in the low momentum region it is as accurate as the derivative expansion at next-to-leading order (corresponding to an effective action quadratic in the derivatives, with a field dependent coefficient).

3 Analysis of the flow equation

There are two features of equation (16) that make it a priori difficult to solve. First, the two functions $J_d^{(3)}(p;\kappa;\rho)$ and $I_d^{(2)}(\kappa;\rho)$, are functionals of the solution $\Gamma_\kappa^{(2)}(p;\rho)$ (see Eq. (6)). Second the different values of p are coupled through the propagator $G_\kappa(p+q)$ entering the calculation of $J_d^{(3)}(p;\kappa;\rho)$. In principle, one should therefore solve equation (16) self-consistently, and simultaneously for all values of p. However, in this section, we shall show that it is possible to make an accurate calculation of $J_d^{(3)}(p;\kappa;\rho)$ and $I_d^{(2)}(\kappa;\rho)$ using approximate propagators. This yields

an approximate version of equation (16) that can be solved for each given value of p. The validity of this approximation will be checked in the next section.

Consider first the function $I_d^{(n)}(\kappa;\rho)$, which does not depend on p. The smoothness of the n-point functions and the fact that $q \leq \kappa$, suggest to perform in the propagators of the right-hand-side of equation (11) an approximation similar to that applied to the other n-point functions, i.e., set $q = 0$. However, in order to maintain the exact one-loop properties of the flow equations, one cannot simply set $q = 0$ in the propagators: rather, one needs to keep a momentum dependence close to that of the free propagators. Thus, we shall use for the propagators entering the calculation of $I_d^{(n)}(\kappa;\rho)$ the following approximate form

$$G_\kappa^{-1}(q;\rho) \approx Z_\kappa q^2 + \Gamma_\kappa^{(2)}(q=0;\rho) + R_\kappa(q), \qquad (17)$$

where

$$Z_\kappa \equiv \left.\frac{\partial \Gamma_\kappa^{(2)}}{\partial q^2}\right|_{q=0,\rho=\rho_0}. \qquad (18)$$

As well known [5], and will be verified in Appendix A, the quantity $\partial\Gamma^{(2)}(q;\rho)/\partial q^2\big|_{q=0}$ depends weakly on ρ. Accordingly, one expects Z_κ to depend weakly on the value chosen for ρ_0. As will be seen in Appendix A, the choice $\rho_0 = 0$ is here the simplest. With the propagator (17), and the function (3) for $R_\kappa(q)$ one can calculate $I_d^{(n)}(\kappa;\rho)$ analytically:

$$I_d^{(n)}(\kappa;\rho) = 2K_d \frac{\kappa^{d+2-2n}}{Z_\kappa^{n-1}} \frac{1}{(1+\hat{m}_\kappa^2(\rho))^n}\left(1 - \frac{\eta_\kappa}{d+2}\right). \qquad (19)$$

In this expression,

$$\eta_\kappa \equiv -\kappa\partial_\kappa \ln Z_\kappa \qquad (20)$$

is the running anomalous dimension and

$$\hat{m}_\kappa^2(\rho) \equiv \frac{\Gamma_\kappa^{(2)}(q=0;\rho)}{\kappa^2 Z_\kappa}, \qquad (21)$$

is a dimensionless, field-dependent, effective mass. The constant K_d is a number resulting from angular integration, $K_d^{-1} \equiv d\ 2^{d-1}\ \pi^{d/2}\ \Gamma(d/2)$ (e.g., $K_3 = 1/(6\pi^2)$). Notice that, for $d > 2$, $I_d^{(2)}(\kappa;\rho) \to 0$ when $\kappa \to 0$.

We shall calculate the function $J_d^{(3)}(p,\kappa;\rho)$ in a similar way, arguing that in this calculation one can assume $p \lesssim \kappa$: the propagator $G_\kappa(p+q;\rho)$ in equation (10) is small as soon as p/κ is large, and one can indeed verify that the function $J_d^{(3)}(p;\kappa;\rho)$ vanishes approximately as κ^2/p^2 for large values of p/κ (see the explicit expressions (40) and (42) given in Appendix B). Thus, in the region where $J_d^{(3)}(p;\kappa;\rho)$ has a significant value, one can use for $G_\kappa(p+q;\rho)$ an expression similar to (17), namely

$$G_\kappa^{-1}(p+q;\rho) \approx Z_\kappa(p+q)^2 + \Gamma_\kappa^{(2)}(0;\rho) + R_\kappa(p+q). \qquad (22)$$

One can then calculate the function $J_d^{(3)}(p;\kappa;\rho)$ analytically (in $d = 3$). The resulting expression is more complicated than that of $I_d^{(2)}(\kappa;\rho)$, equation (19). It is given in Appendix B (see also [20]). Observe that the regulator in equation (3) is not analytic at $q \sim \kappa$. This generates non analyticities in $J_d^{(3)}(p;\kappa;\rho)$; but these occur only in the third derivative with respect to p, at $p = 0$ and at $p = 2\kappa$ (cf. the odd powers of $\bar{p}$ in Eqs. (40–43)), and they play no role at the present level of approximation.

With the approximations just discussed, $I_d^{(2)}(\kappa;\rho)$ and $J_d^{(3)}(p;\kappa;\rho)$ depend only on quantities that enter the flow equation at $p = 0$, namely $\hat{m}_\kappa^2(\rho)$, Z_κ and η_κ. As we discuss in Appendix A, these quantities can be obtained from a modified version of the Local Potential approximation [7] that we call the LPA'. The strategy to solve equation (16) consists then in two steps: one first solves the LPA' to get $\hat{m}_\kappa^2(\rho)$, Z_κ and η_κ; then, for each value of p, one solves equation (16) with the kernels $I_d^{(2)}(\kappa;\rho)$ and $J_d^{(3)}(p;\kappa;\rho)$ that are calculated with $\hat{m}_\kappa^2(\rho)$, Z_κ and η_κ determined from the LPA'.

Note that, generally, the flow of Σ gets strongly suppressed below some non vanishing value of κ. This can be inferred from the properties of the functions $I_3^{(2)}(\kappa;\rho)$ and $J_3^{(3)}(p;\kappa;\rho)$ discussed above, and it will be verified explicitly on the numerical results presented in the next section. In fact, the flow of Σ receives two contributions: the first involves the external momentum $p \neq 0$ and is suppressed when $\kappa \lesssim p$ ($J_3^{(3)}(p;\kappa;\rho)$ vanishes rapidly when κ becomes smaller than p); the other contribution is independent of p and, at criticality, is suppressed for $\kappa \lesssim \kappa_c \sim u/10$ (see Appendix A, and in particular Fig. 6). Accordingly, one expects the flow to stop when κ reaches the smallest of κ_c and p.

The function $\Gamma_\kappa^{(2)}(p;\rho)$ exhibits a simple scaling behavior. Consider for simplicity the zero field case $\rho = 0$, and the ratio

$$\frac{p^2 + \Gamma_\kappa^{(2)}(0;\rho=0) + \Sigma_\kappa(p;\rho=0)}{\Gamma_\kappa^{(2)}(0;\rho=0)} = f\left(\frac{p}{\kappa}, \frac{p}{u}\right). \qquad (23)$$

At criticality, and in the scaling regime where $p, \kappa \ll u$, we expect f to become independent of u, and therefore a function of p/κ only. As will be shown in the next section, the solution of equation (16) verifies this property. Note that this scaling behavior is reproduced only when including a renormalization factor Z_κ whose flow is determined consistently from that of $\partial\Sigma_\kappa/\partial p^2$ for $p < \kappa$, as obtained from equation (16). This calculation of Z_κ is explained in Appendix A. We have tested the consequence of setting $Z_\kappa = 1$ in the propagators (17) and (22), corresponding to the Local Potential approximation (as opposed to the LPA'). Doing so does not alter the self-energy in any significant way when $p \gtrsim u$, but in the IR regime, the scaling behavior is only approximate.

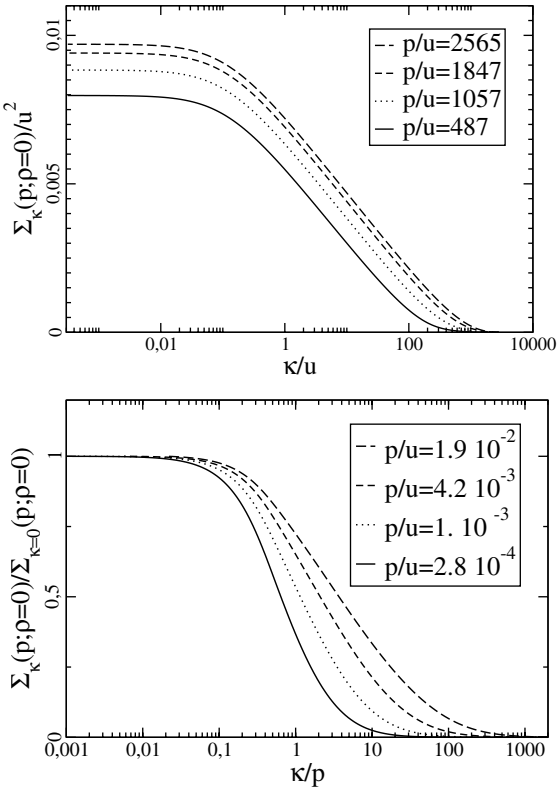

Fig. 1. Top: $\Sigma_\kappa(p;\rho=0)/u^2$ as a function of κ/u for various values of $p \gg u$. The flow stops at $\kappa \lesssim \kappa_c \sim u/10$. Bottom: $\Sigma_\kappa(p;\rho=0)/\Sigma(p=0;\rho=0)$ as a function of κ/p for various values of $p \ll u$. The flow stops at $\kappa \lesssim p/10$.

4 Numerical results and discussion

We now turn to the numerical solution of the flow equation for $\Sigma_\kappa(p;\rho)$, at $d=3$ and at criticality. Our goal is to assess the quality of the approximation scheme, and there are two aspects that we shall examine. First, since the strategy described in the previous section provides only an approximate solution to equation (16), we shall estimate by how much this approximate solution differs from the exact solution of this equation. Second, since equation (16) itself is only the LO approximation of the method described in [14], we shall compare our results with known ones concerning the self-energy of the scalar model at criticality.

Let us start by considering general properties of the flow, and verify in particular that it stops when κ is small enough, i.e., before reaching the value $\kappa = 0$. Figure 1 displays the self-energy, $\Sigma_\kappa(p;\rho=0)$ as a function of κ/u, for different values of p. Calculations are made for $u/\Lambda = 3.54 \times 10^{-4}$ (this value is small enough to guarantee that the results are independent of Λ). The top panel of Figure 1 shows the flow of $\Sigma_\kappa(p;\rho=0)$ for values of p in the UV regime, i.e., $p \gg \kappa_c \sim u/10$; for all the considered values of p the flow stops at κ_c. The bottom panel of Figure 1 presents the flow of the self-energy when p is in the IR regime, i.e., when $p \ll \kappa_c$. In this case, we have divided $\Sigma_\kappa(p;\rho=0)$ by its physical value $\Sigma(p;\rho=0) \equiv \Sigma_{\kappa=0}(p;\rho=0)$, in order to make it more obvious that the flow only stops when $\kappa \lesssim p$.

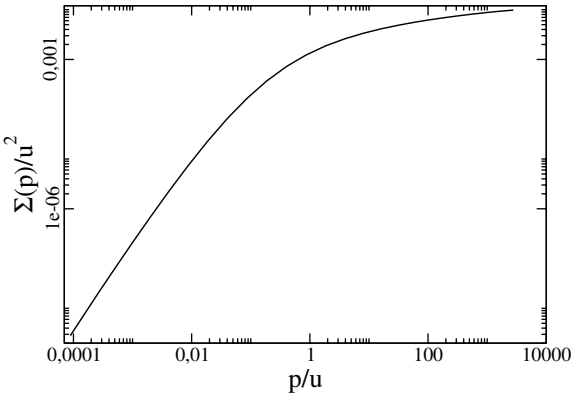

Fig. 2. $\Sigma(p)/u^2$, in $d=3$, at criticality and zero external field, as a function of p/u.

We now turn to $\Sigma(p) \equiv \Sigma_{\kappa=0}(p;\rho=0)$, the physical self-energy in vanishing external field, displayed in Figure 2 as a function of p/u, and discuss its behavior in the various momentum regions: $p \gg u$, $p \ll u$, $p \sim \kappa_c \sim u/10$. We have checked that the curve in Figure 2, i.e., $(1/u^2)\Sigma(p/u)$, is "universal", i.e., independent of u and Λ, provided u/Λ is small enough.

In the perturbative regime ($p \gg u$), one expects $\Sigma(p) \approx (u^2/96\pi^2)\log(p/u)$. In Appendix C we show that the analytical solution of equation (16) preserves this behavior, although the coefficient in front of the logarithm is $(u^2/9\pi^4)$, 8% larger (the LO approximation does not include all the 2-loop perturbative diagrams exactly). Our approximate numerical solution reproduces this result. As explained in [14], at the NLO of our approximation scheme, which is beyond the scope of the present paper, the contribution of the 2-loops diagrams would be exactly included and the correct prefactor $(u^2/96\pi^2)$ would be recovered.

In the IR region ($p \ll u$) we expect the self-energy to behave as

$$p^2 + \Sigma(p) = Ap^{2-\eta^*}, \tag{24}$$

where η^* is the anomalous dimension. By analyzing the small momentum behavior o $\Sigma(p)$, we get numerically $\eta^* = 0.05218$. An alternative way to determine η is to extract it from the κ dependence of Z_κ (see Eq. (20)). As recalled in Appendix A, in the critical regime, i.e., when $\kappa \lesssim \kappa_c$, $Z_\kappa \propto \kappa^{-\eta^*}$, with $\eta^* = 0.05220$ the fixed point value of η_κ (see Fig. 6). It is also shown in Figure 6 in Appendix A that the quantity $\Gamma^{(2)}_\kappa(p=0;\rho=0)/(\kappa^2 Z_\kappa)$ goes to a fixed point, which confirms the behavior of $\Gamma^{(2)}_\kappa(p=0;\rho=0) \sim \kappa^{2-\eta}$ expected in the scaling regime.

We have performed a more stringent test of scaling by studying the function $(p^2+\Sigma_\kappa(p))/(Z_\kappa p^2)$. This function is displayed in Figure 3 as a function of p/κ. By definition of Z_κ (see Eq. (18)), when κ is kept fixed and $p \to 0$, this function goes to one. Furthermore, as explained before, in the scaling regime $p, \kappa \ll u$, one expects this function to depend on p/κ only, which is

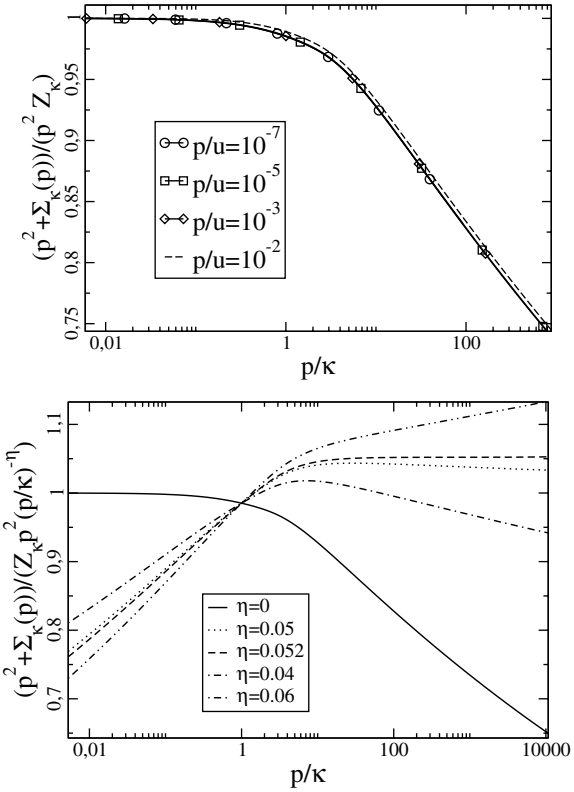

Fig. 3. The ratio $(p^2 + \Sigma_\kappa(p))/(Z_\kappa p^2)$ as a functio of p/κ. Bottom: the same ratio divided by $(p/\kappa)^{-\eta^*}$.

indeed well verified, as can be seen on the top panel of Figure 3; it is only for values of p which are not small enough ($p/u = 10^{-2}$, corresponding to the dashed line) that violation of this scaling start to become significant. Moreover, as can be seen on the figure, $p^2 + \Sigma_\kappa(p)$ is well approximated by $Z_\kappa p^2$ for all $p \lesssim \kappa$. In the bottom panel of Figure 3, we have plotted the ratio $(p^2 + \Sigma_\kappa(p))/(Z_\kappa p^2)$ divided by $(p/\kappa)^{-\eta^*}$. Recall that when $\kappa \ll p \ll \kappa_c$, one expects $p^2 + \Sigma_\kappa(p) \sim p^{2-\eta^*}$, while $Z_\kappa \sim \kappa^{-\eta^*}$ when $\kappa \lesssim \kappa_c$. Therefore when $1 \ll p/\kappa \ll \kappa_c/\kappa$, one expects $(p^2 + \Sigma_\kappa(p))/(Z_\kappa p^2) \sim (p/\kappa)^{-\eta^*}$, so that the quantity which is plotted should be constant. As seen in the bottom panel of Figure 3, this is indeed the case for the value $\eta^* = 0.05219$, which confirms the coherence of the whole calculation.

Our estimate for the anomalous dimension, $\eta^* \approx 0.052$ is to be compared with the results $\eta^* = 0$, $\eta^* = 0.044$ and $\eta^* = 0.033$ obtained with the derivative expansion at LO, NLO and NNLO, respectively [5, 12, 24], and $\eta^* = 0.0335 \pm 0.0025$ from the resummed 7 loop calculation of reference [28]. Note however that the values quoted above do not correspond all to the same regulator, and in general the results depend slightly on the choice of the regulator. The value $\eta^* = 0.044$ obtained with the derivative expansion at NLO results from an optimization within a family of exponential regulators; if instead the optimization is done within the family of θ-regulators considered in [24], the result is 0.047; with the regulator of the the present paper one gets $\eta^* = 0.05$ (see [24] for a thorough discussion of this point). We note finally that the value of η^* obtained here is slightly larger than that obtained in [19] using a different version of the LPA' than that used here. In fact, the present version of the LPA' is close to the derivative expansion in next-to-leading order.

We turn now to the intermediate momentum region, which we shall probe with a quantity which is very sensitive to the cross-over between the two regimes just studied:

$$\Delta\langle\phi^2\rangle = \int \frac{d^3p}{(2\pi)^3} \left(\frac{1}{p^2 + \Sigma(p)} - \frac{1}{p^2}\right). \qquad (25)$$

As shown for instance in [25], the integrand in equation (25) is peaked at $p \sim \kappa_c$ (in fact it takes significant values only in the region $10^{-3} \lesssim p/u \lesssim 10$). This quantity has been much studied recently for a scalar model with $O(2)$ symmetry because it determines then the shift of the critical temperature of the weakly repulsive Bose gas [29]. For the simple scalar model studied in this paper, lattice calculations measure [30] $\Delta\langle\phi^2\rangle/u = -(4.95 \pm 0.41) \times 10^{-4}$ while the "7 loop" resummed calculation of reference [31] yields $\Delta\langle\phi^2\rangle/u = -(4.86 \pm 0.45) \times 10^{-4}$. With the present numerical solution, one gets $\Delta\langle\phi^2\rangle/u = -5.45 \times 10^{-4}$. This is only slightly larger than the value $\Delta\langle\phi^2\rangle/u = -5.03 \times 10^{-4}$ obtained in the next-to-leading order of the scheme presented in [19, 20].

We conclude that with the LO of the present approximation scheme, we obtain an accurate description of the self-energy in the entire range of momenta. Since we have solved only approximately equation (16), it remains to study by how much the solution that we have obtained differs from the exact solution of equation (16). We have already indications about the accuracy of the approximation both in the UV and in the IR. In the UV, we reproduce the expected result (which differs by 8% from the exact 2-loop result). We also loose the 2-loop accuracy with which the effective potential could be obtained in the LO of our scheme, by using LPA' propagators. In the IR, we have already commented on the quality of the value that one obtains for the anomalous dimension. As a further test, we have recalculated $I_3^{(2)}(\kappa;\rho)$ and $J_3^{(3)}(p;\kappa;\rho)$ using, instead of the LPA' propagators, the propagators (6) in which $\Gamma_\kappa^{(2)}(p;\rho)$ is the 2-point function that has been obtained in this section by approximately solving equation (16).

In Figure 4 we plot the ratio of the function $I_3^{(2)}(\kappa;\tilde{\rho})$ ($\tilde{\rho} \sim \rho/\kappa$, see Eq. (32)) calculated with the propagator obtained from the numerical integration of the flow equation divided by the function given by equation (11). One can see that the smaller the value of κ, the larger the difference, and that the main error is for values of $\tilde{\rho}$ around the minimum $\tilde{\rho}_{min}$ of the effective potential ($\tilde{\rho}_{min}$ goes from 1.8 to 3 as κ runs from Λ to 0). Nevertheless, the difference stabilizes for small enough κ and it never exceeds 4%. The bottom panel of Figure 4 shows the comparison of the two curves in the worst situation, i.e., for small values of κ, as a function of $\tilde{\rho}$: the curves are hardly distinguishable.

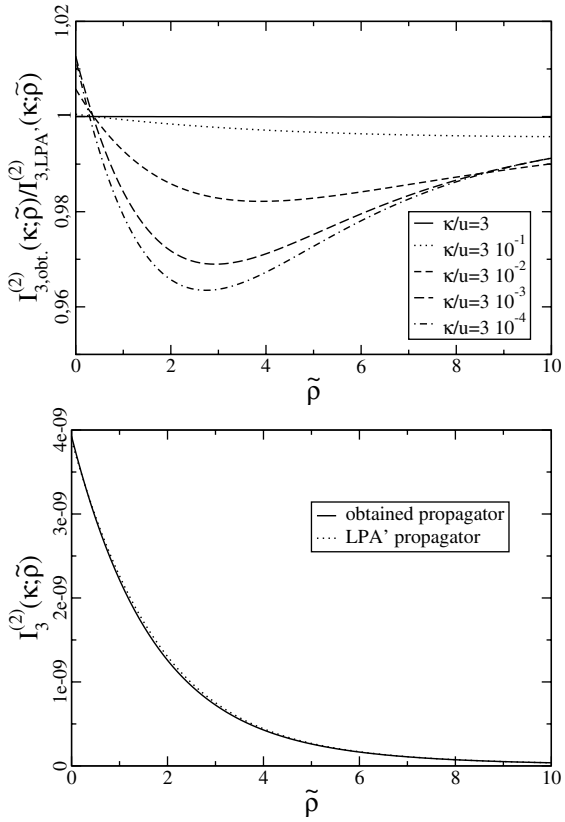

Fig. 4. Top: the ratio of the function $I_3^{(2)}(\kappa;\tilde{\rho})$ calculated with the obtained numerical propagator and with the approximate LPA' propagator (as explained in the text), as a function of $\tilde{\rho}$, for different values of κ/u. Bottom: the function $I_3^{(2)}(\kappa;\tilde{\rho})$ as a function of $\tilde{\rho}$, for $\kappa/u = 3\times10^{-4}$, calculated with the approximate propagator (dotted line) and with the obtained numerical propagator (solid line).

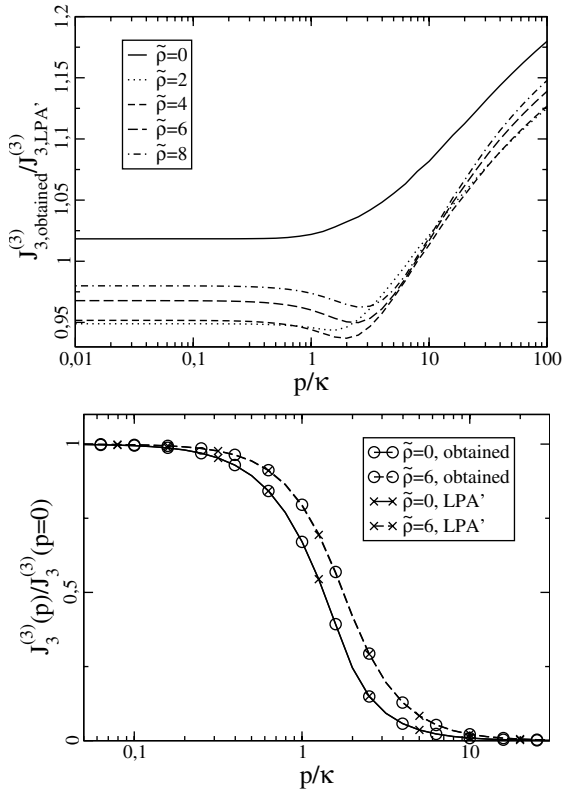

Fig. 5. Top: the ratio of the function $J_3^{(3)}(p;\kappa;\tilde{\rho})$ calculated with the obtained numerical propagator and with the approximate propagators, as a function of p/κ, for $\kappa/u = 3\times10^{-4}$ and for different values of $\tilde{\rho}$. Bottom: the function $J^{(3)}(p;\kappa;\tilde{\rho})/J_3^{(3)}(p=0;\kappa;\tilde{\rho})$ calculated with the obtained numerical propagator compared to that calculated with the approximate propagators, as a function of p/κ, for $\kappa/u = 3\times10^{-4}$ and for different values of $\tilde{\rho}$.

The same analysis is repeated for $J_3^{(3)}$. Again, it is only for small values of κ that the two functions differs. In the top panel of Figure 5 we display the ratio of the function $J_3^{(3)}$ calculated respectively with the obtained (numerator) and the approximate (denominator) propagators, for $\kappa/u = 3\times10^{-4}$, for various values of $\tilde{\rho}$. The difference can be large, but only in the region ($p \gg \kappa$) where the function $J_3^{(3)}$ itself is very small. In the region where the function is non negligeable, the difference between the two calculations never exceeds 5%. As was the case for $I_3^{(2)}$, the largest error occurs for values of $\tilde{\rho}$ near the minimum of the potential. In the bottom panel of Figure 5, we plot the two functions for the same values of κ and $\tilde{\rho}$ as in the top panel: the difference between the two calculations of $J_3^{(3)}$ is invisible on such a plot.

5 Conclusions and perspectives

We have demonstrated in this paper that the method proposed in [14] allows for concrete numerical applications. We have calculated the self-energy of the scalar model, at the LO of the approximation scheme, at criticality, at zero external field, in $d = 3$, and have obtained accurate results over the whole range of momenta. Already at this level of approximation the results obtained compare well with those of more elaborate techniques. Worth emphasizing is the fact that the scaling behavior of the self-energy is accurately reproduced: not only do we get a reasonable estimate of the anomalous dimension, but the entire dependence of the self-energy on the momentum and the cut-off follows accurately the expected scaling behavior.

In the present paper, whose main objective was to confirm the applicability of the method to a concrete calculation, we solved approximately the flow equation (16). However, several tests suggest that this approximate solution differs in fact very little from the complete solution of (16). Of course, a definite statement concerning the error made in the present calculation can only come from a comparison with the exact solution. This, we believe, is within reach. Similarly, work is in progress to test the convergence of the procedure by calculating the next-to-leading order contribution.

The method of reference [14] builds on our previous works on the same subject [19, 20]. The results presented in this paper indicate that it is both conceptually simpler, and numerically more accurate, than the method which we have developed in [19, 20]. It offers the possibility of applications to a variety of non-perturbative problems, where the knowledge of the momentum dependence of n-point functions is necessary. Even the approximate treatment presented in this paper could constitute an interesting starting point in situations where only a semi-quantitative description would be valuable.

We would like to thank Hugues Chaté, Bertrand Delamotte and Diego Guerra for many fruitful discussions. Ramón Méndez-Galain and Nicolás Wschebor are grateful for the hospitality of the ECT* in Trento where part of this work has been carried out.

Appendix A: The p = 0 sector

As discussed in the main text, our approximate solution of equation (16) builds on the prior determination of quantities that are independent of momentum. These are calculated using a variant of the derivative expansion that we describe in this appendix. The derivative expansion is usually [7] formulated in terms of an ansatz for the running effective action $\Gamma_\kappa[\phi]$, including terms up to a given number of derivatives of the field. Its leading order, the so-called local potential approximation (LPA), assumes that the effective action has the form:

$$\Gamma_\kappa^{LPA}[\phi] = \int d^dx \left\{ \frac{1}{2}\partial_\mu\phi_a\partial_\mu\phi_a + V_\kappa(\rho) \right\} \qquad (26)$$

where the derivative term is simply the one appearing in the classical action, and $V_\kappa(\rho)$ is the effective potential. In the next-to-leading order (NLO), one assumes [1]

$$\Gamma_\kappa^{NLO}[\phi] = \int d^dx \left\{ \frac{Z_\kappa(\rho)}{2}\partial_\mu\phi_a\partial_\mu\phi_a + V_\kappa(\rho) \right\}. \quad (27)$$

An interesting improvement of the LPA, which we refer to as the LPA', is a simplified version of the NLO that consists in ignoring the ρ-dependence of $Z_\kappa(\rho)$, i.e., in choosing $Z_\kappa = Z_\kappa(\rho_0)$ where ρ_0 is a given value of ρ, usually taken to be the running minimum of the potential. In the LPA' one solves simultaneously the flow equations for both the effective potential $V_\kappa(\rho)$ (a partial differential equation in κ and ρ) and for Z_κ. In this approximation, the inverse propagator takes the form of equation (17): $G_\kappa^{-1}(q^2;\phi) = Z_\kappa q^2 + V_\kappa''(\phi) + R_\kappa(q)$, with $V_\kappa''(\phi) = d^2V_\kappa/d\phi^2$. The LPA' allows for a non-trivial anomalous dimension, which is determined from the cut-off dependence of Z_κ (see Eq. (20) and Ref. [1]).

The procedure followed in this paper to determine the field renormalisation constant Z_κ differs slightly from that used in [19]. This is because, as explained in Section 3, we need the calculation of Z_κ to be consistent with the approximate equation (16) for the 2-point function. This is essential to get the proper scaling behavior of $\Gamma_\kappa^{(2)}(p;\rho)$ at small momenta. We set (cf. Eq. (18)):

$$Z_\kappa(\rho) \equiv 1 + \left.\frac{\partial\Sigma_\kappa(p;\rho)}{\partial p^2}\right|_{p=0}, \qquad (28)$$

where $\Sigma_\kappa(p;\rho)$ is defined in equation (15). The flow equation obeyed by $Z_\kappa(\rho)$ reads

$$\kappa\partial_\kappa Z_\kappa(\rho) = \left.\frac{\partial J_d^{(3)}(p^2,\rho)}{\partial p^2}\right|_{p=0} \left(\frac{\partial^3 V}{\partial\phi^3}\right)^2 + 2I_d^{(3)}(\rho)\frac{\partial^3 V}{\partial\phi^3}\frac{\partial Z_\kappa(\rho)}{\partial\phi} - \frac{1}{2}I_d^{(2)}(\rho)\frac{\partial^2 Z_\kappa(\rho)}{\partial\phi^2}, \qquad (29)$$

which follows immediately from equation (16) for $\Gamma_\kappa^{(2)}(p;\rho)$. Knowing the solution of this equation we can calculate η_κ from equations (20) and (18). At this point, it is convenient to choose $\rho_0 = 0$. Then the expression of η_κ that one deduces from equation (29) simplifies into:

$$\eta_\kappa = \frac{1}{2}I_d^{(2)}(\rho=0)\frac{1}{Z_\kappa}\left.\frac{\partial^2 Z_\kappa(\rho)}{\partial\phi^2}\right|_{\rho=0}. \qquad (30)$$

Since $I_d^{(2)}(\rho=0)$ depends explicitly on Z_κ and η_κ (see Eq. (19)), equation (30) is in fact a self-consistent equation for η_κ.

The solution of the LPA' is well documented in the literature (see e.g. [7, 24]). In practice, we work with dimensionless quantities. We set:

$$v_\kappa(\tilde\rho) \equiv K_d^{-1}\kappa^{-d}V_\kappa(\rho), \qquad \chi(\tilde\rho) \equiv \frac{Z_\kappa(\rho)}{Z_\kappa}, \qquad (31)$$

with

$$\tilde\rho \equiv K_d^{-1}\, Z_\kappa\, \kappa^{2-d}\, \rho, \qquad (32)$$

and K_d is given after equation (21). We solve the equation for the derivative of the potential with respect to $\tilde\rho$, i.e., $w_\kappa(\tilde\rho) \equiv \partial_{\tilde\rho}v_\kappa(\tilde\rho)$, rather than that for the effective potential itself. This reads (from now on we stick to $d = 3$):

$$\kappa\partial_\kappa w_\kappa = -(2-\eta_\kappa)w_\kappa + (1+\eta_\kappa)\tilde\rho w_\kappa' - \left(1-\frac{\eta_\kappa}{5}\right)\left(\frac{(N-1)w_\kappa'}{(1+w_\kappa)^2} + \frac{3w_\kappa' + 2\tilde\rho w_\kappa''}{(1+w_\kappa+2\tilde\rho w_\kappa')^2}\right), \qquad (33)$$

where $w_\kappa' = \partial_{\tilde\rho}w_\kappa(\tilde\rho)$, $w_\kappa'' = \partial_{\tilde\rho}^2 w_\kappa(\tilde\rho)$. Equation (33) is solved starting from the initial condition at $\kappa = \Lambda$:

$$w_\kappa(\tilde\rho, \kappa=\Lambda) = \hat m_\Lambda^2 + \hat g_\Lambda\tilde\rho, \qquad (34)$$

where $\hat m_\Lambda$ and $\hat g_\Lambda$ are related to the parameters r and u of the classical action (1) by

$$\hat m_\Lambda^2 = \frac{r}{\Lambda^2}, \qquad \hat g_\Lambda = \frac{u}{\Lambda}\frac{K_3}{3}, \qquad (35)$$

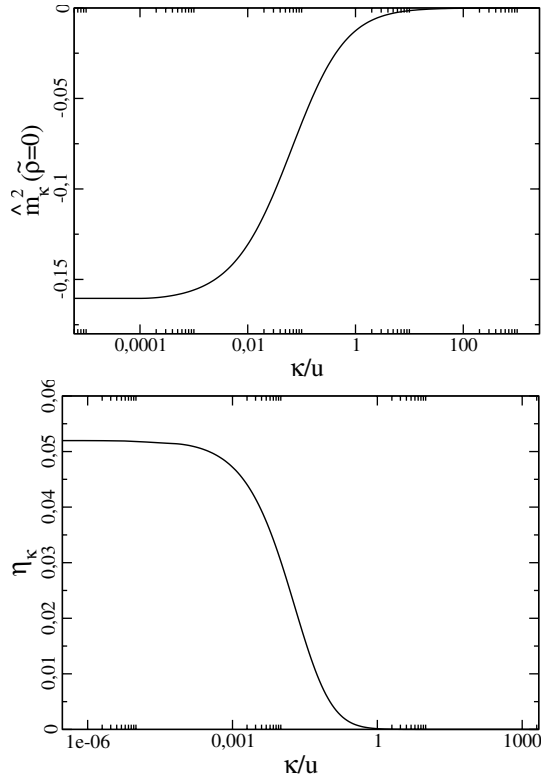

Fig. 6. The dimensionless mass $\hat{m}^2_\kappa(\tilde{\rho}=0) = \partial_{\tilde{\rho}} v_\kappa(\tilde{\rho}=0)$ (top) and the anomalous dimension η_κ (bottom) as a function of κ/u. These quantities were obtained by solving the LPA' equations, with $u/\Lambda = 3.54 \times 10^{-4}$ and the parameter r adjusted to be at criticality.

and the parameter r is adjusted to be at criticality. Together with equation (33), we solve the equation for $\chi_\kappa(\tilde{\rho} > 0)$, which reads

$$\kappa\partial_\kappa\chi_\kappa = \eta_\kappa\chi_\kappa + (1+\eta_\kappa)\tilde{\rho}\chi'_\kappa - 2\tilde{\rho}\frac{(3w'_\kappa + 2\tilde{\rho}w''_\kappa)^2}{(1+w_\kappa+2\tilde{\rho}w'_\kappa)^4} + 8\tilde{\rho}\chi'_\kappa(1-\frac{\eta_\kappa}{5})\frac{(3w'_\kappa+2\tilde{\rho}w''_\kappa)}{(1+w_\kappa+2\tilde{\rho}w'_\kappa)^3} - (1-\frac{\eta_\kappa}{5})\frac{\chi'_\kappa+2\tilde{\rho}\chi''_\kappa}{(1+w_\kappa+2\tilde{\rho}w'_\kappa)^2}, \quad (36)$$

where $\chi'_\kappa = d\chi_\kappa/d\tilde{\rho}$. The initial condition is $\chi_\kappa(\tilde{\rho}=0) = 1$ for all κ, which follows from the definition of Z_κ, equation (18). Finally, for η_κ we have simply:

$$\eta_\kappa = \frac{\chi'_\kappa(0)}{(1+w_\kappa(0))^2 + \chi'_\kappa(0)/5}. \quad (37)$$

For the sake of illustration, we present in Figure 6 the LPA' solutions for $\hat{m}^2_\kappa(\tilde{\rho}=0)$ (defined in Eq. (21)) and η_κ, as a function of κ/u. The calculations have been done with $u/\Lambda = 3.54 \times 10^{-4}$, but the curves are independent of this choice, provided u/Λ remains small. One can verify that the the crossover between the UV and IR regimes occurs around $\kappa_c \sim u/10$. The fixed point value of η_κ is $\eta^* = \eta_{\kappa\to 0} \approx 0.05220$, and that of $\hat{m}^2_\kappa(\tilde{\rho}=0)$, –0.1608.

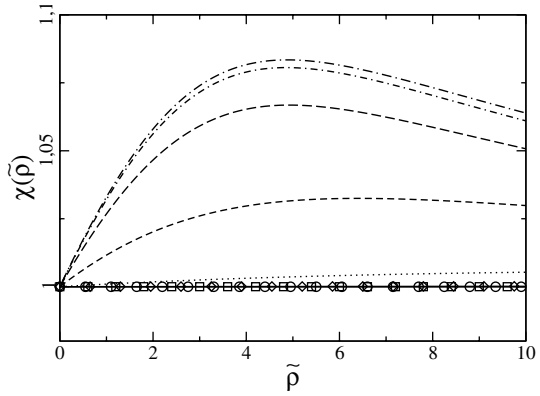

Fig. 7. The dimensionless function $\chi(\tilde{\rho})$ defined in eq. (31), for various values of $\kappa/u = 3\times 10^n$, with $n = 2$ (circles), $n = 1$ (squares), $n = 0$ (diamonds), $n = -1, \cdots, -5$ from bottom to top.

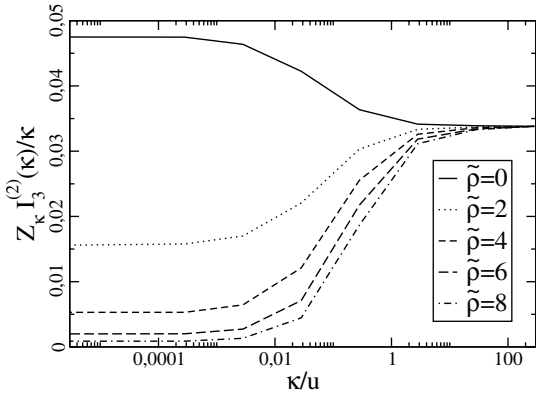

Fig. 8. The function $Z_\kappa I_3^{(2)}(\kappa;\tilde{\rho})/\kappa$ as a function of κ/u, for different values of $\tilde{\rho}$.

Figure 7 illustrates the ρ-dependence of the renormalization factor $Z_\kappa(\rho)$ (see Eq. (31)). This dependence is completely negligible when $\kappa \gtrsim \kappa_c \sim u/10$, and never exceeds 8%.

Appendix B: The functions $I_3^{(2)}(\kappa;\rho)$ and $J_3^{(3)}(p;\kappa;\rho)$

In this appendix we provide details about the functions $I_3^{(2)}(\kappa;\rho)$ and $J_3^{(3)}(p;\kappa;\rho)$ calculated with the propagators (17) and (22) respectively.

Consider first the function $I_3^{(2)}(\kappa;\rho)$, defined in equation (11), and whose explicit expression is given in equation (19). The variation of $I_3^{(2)}(\kappa;\rho)$ with κ is dominated by the explicit linear κ dependence and the κ-dependence of the renormalization factor Z_κ. The function

$$\frac{Z_\kappa I_3^{(2)}(\kappa;\rho)}{\kappa} = 2K_3\frac{1}{(1+\hat{m}^2_\kappa(\tilde{\rho}))^2}\left(1-\frac{\eta_\kappa}{5}\right), \quad (38)$$

displayed in Figure 8, illustrates the remaining dependence on κ and $\tilde{\rho}$.

$$J_3^{(3)}(p;\kappa;\rho) = \frac{1}{\kappa Z_\kappa^2(2\pi)^2}\frac{1}{(1+\hat{m}_\kappa^2)^2}\int_0^1 d\bar{q}\bar{q}^2\int_{-1}^1 d(\cos\gamma) \times\frac{(2-\eta+\eta\bar{q}^2)}{\Theta(1-\bar{q}^2-\bar{p}^2+2\bar{q}\bar{p}\cos\gamma)+(\bar{q}^2+\bar{p}^2-2\bar{q}\bar{p}\cos\gamma)\Theta(\bar{q}^2+\bar{p}^2-2\bar{q}\bar{p}\cos\gamma-1)+\hat{m}_\kappa^2}. \tag{39}$$

a) $\bar{p}>2, \hat{m}_\kappa^2<0$.

$$\begin{aligned} J_3^{(3)}(p;\kappa;\tilde{\rho}) &= \frac{1}{\kappa Z_\kappa^2(2\pi)^2}\frac{1}{(1+\hat{m}_\kappa^2)^2}\left\{2+\frac{\eta}{2}\left(-\frac{5}{3}+\bar{p}^2-3\hat{m}_\kappa^2\right)\right. \\ &+\frac{1}{2\bar{p}}\left[-1+\frac{\eta}{4}+\left(\bar{p}+\sqrt{-\hat{m}_\kappa^2}\right)^2\left(1-\frac{\eta}{2}+\frac{\eta}{4}\left(\bar{p}+\sqrt{-\hat{m}_\kappa^2}\right)^2\right)\right]\log\left(\frac{\bar{p}-1+\sqrt{-\hat{m}_\kappa^2}}{\bar{p}+1+\sqrt{-\hat{m}_\kappa^2}}\right) \\ &\left.+\frac{1}{2\bar{p}}\left[-1+\frac{\eta}{4}+\left(\bar{p}-\sqrt{-\hat{m}_\kappa^2}\right)^2\left(1-\frac{\eta}{2}+\frac{\eta}{4}\left(\bar{p}-\sqrt{-\hat{m}_\kappa^2}\right)^2\right)\right]\log\left(\frac{\bar{p}-1-\sqrt{-\hat{m}_\kappa^2}}{\bar{p}+1-\sqrt{-\hat{m}_\kappa^2}}\right)\right\} \\ &= \frac{1}{\kappa Z_\kappa^2(2\pi)^2}\frac{1}{(1+\hat{m}_\kappa^2)^2}\left\{\frac{4}{\bar{p}^2}\left(\frac{1}{3}-\frac{\eta}{15}\right)+\frac{4}{\bar{p}^4}\left(\frac{1}{15}-\frac{\eta}{105}-\frac{\hat{m}_\kappa^2}{3}+\frac{\eta\hat{m}_\kappa^2}{15}\right)+\mathcal{O}(1/(\bar{p}^6))\right\}. \end{aligned} \tag{40}$$

b) $\bar{p}\le 2, \hat{m}_\kappa^2<0$.

$$\begin{aligned} J_3^{(3)}(p;\kappa;\tilde{\rho}) &= \frac{1}{\kappa Z_\kappa^2(2\pi)^2}\frac{1}{(1+\hat{m}_\kappa^2)^2}\left\{-1+\frac{\eta}{4}+\frac{\eta\hat{m}_\kappa^2}{4}+\bar{p}\left(\frac{3}{2}-\frac{\eta}{8}-\frac{7\eta\hat{m}_\kappa^2}{8}\right)-\frac{3\eta}{4}\bar{p}^2\right. \\ &+\frac{25\eta}{48}\bar{p}^3+\frac{1}{1+\hat{m}_\kappa^2}\left(\frac{4}{3}-\frac{4\eta}{15}-\bar{p}+\frac{\eta}{3}\bar{p}^2+\left(\frac{1}{12}-\frac{\eta}{6}\right)\bar{p}^3+\frac{\eta}{120}\bar{p}^5\right) \\ &+\frac{1}{2\bar{p}}\left[1-\frac{\eta}{4}-\left(\bar{p}+\sqrt{-\hat{m}_\kappa^2}\right)^2\left(1-\frac{\eta}{2}+\frac{\eta}{4}\left(\bar{p}+\sqrt{-\hat{m}_\kappa^2}\right)^2\right)\right]\log\left(\frac{\bar{p}+1+\sqrt{-\hat{m}_\kappa^2}}{1+\sqrt{-\hat{m}_\kappa^2}}\right) \\ &\left.+\frac{1}{2\bar{p}}\left[1-\frac{\eta}{4}-\left(\bar{p}-\sqrt{-\hat{m}_\kappa^2}\right)^2\left(1-\frac{\eta}{2}+\frac{\eta}{4}\left(\bar{p}-\sqrt{-\hat{m}_\kappa^2}\right)^2\right)\right]\log\left(\frac{\bar{p}+1-\sqrt{-\hat{m}_\kappa^2}}{1-\sqrt{-\hat{m}_\kappa^2}}\right)\right\} \\ &= \frac{1}{\kappa Z_\kappa^2(2\pi)^2}\frac{1}{(1+\hat{m}_\kappa^2)^2}\left\{\frac{4}{3(1+\hat{m}_\kappa^2)}\left(1-\frac{\eta}{5}\right)-\frac{2}{3(1+\hat{m}_\kappa^2)^2}\bar{p}^2\right. \\ &\left.+\frac{2+\eta-2\hat{m}_\kappa^2+\eta\hat{m}_\kappa^2}{6(1+\hat{m}_\kappa^2)^3}\bar{p}^3-\frac{2(1+\eta-5\hat{m}_\kappa^2+\eta\hat{m}_\kappa^2)}{15(1+\hat{m}_\kappa^2)^4}\bar{p}^4+\mathcal{O}(\bar{p}^5)\right\}. \end{aligned} \tag{41}$$

c) $\bar{p}>2, m_\kappa^2\ge 0$.

$$\begin{aligned} J_3^{(3)}(p;\kappa;\tilde{\rho}) &= \frac{1}{\kappa Z_\kappa^2(2\pi)^2}\frac{1}{(1+\hat{m}_\kappa^2)^2}\left\{2+\frac{\eta}{2}\left(-\frac{5}{3}+\bar{p}^2-3\hat{m}_\kappa^2\right)\right. \\ &+\frac{1}{\bar{p}}\left[\left(-1+\frac{\eta}{4}+(\bar{p}^2-\hat{m}_\kappa^2)\left(1-\frac{\eta}{2}+\frac{\eta}{4}(\bar{p}^2-\hat{m}_\kappa^2)\right)-\eta\hat{m}_\kappa^2\bar{p}^2\right)\frac{1}{2}\log\left(\frac{(\bar{p}-1)^2+\hat{m}_\kappa^2}{(\bar{p}+1)^2+\hat{m}_\kappa^2}\right)\right. \\ &\left.\left.-2\hat{m}_\kappa\bar{p}\left(1-\frac{\eta}{2}+\frac{\eta}{2}(\bar{p}^2-\hat{m}_\kappa^2)\right)\left(\mathrm{Arctan}\left(\frac{\hat{m}_\kappa}{\bar{p}-1}\right)-\mathrm{Arctan}\left(\frac{\hat{m}_\kappa}{\bar{p}+1}\right)\right)\right]\right\} \\ &= \frac{1}{\kappa Z_\kappa^2(2\pi)^2}\frac{1}{(1+\hat{m}_\kappa^2)^2}\left\{\frac{4}{\bar{p}^2}\left(\frac{1}{3}-\frac{\eta}{15}\right)\right. \\ &\left.+\frac{1}{105\,\bar{p}^4}\left(7-35\hat{m}_\kappa^2+\eta(-1+7\hat{m}_\kappa^2)\right)+\mathcal{O}(1/(\bar{p}^6))\right\} \end{aligned} \tag{42}$$

Consider next $J_3^{(3)}(p;\kappa;\rho)$, defined in equation (10). Using the LPA' propagators of equations (17) and (22) one can calculate it analytically. One first makes the changes of variables $\bar{p}=p/\kappa, \bar{q}=q/\kappa$ and $\cos\gamma = p.q/p\ q$, and then perform the integral over the remaining angular variables. One gets then

See equation (39) above.

To perform the integral over $\cos\gamma$ one needs to consider the various domains defined by the Θ functions. It is then convenient to separate the calculation in two different regions: $\bar{p}>2$ and $\bar{p}\le 2$, and this for the two possible signs of $\hat{m}_\kappa^2$ (see also [19]). The calculation is then done by first integrating over $\cos\gamma$; the remaining integration over $\bar{q}$ can be done by making first an integration by parts to get a rational function, that is then decomposed into simple fractions. One finally gets (the dependence on $\tilde{\rho}$ is entirely contained in $\hat{m}_\kappa(\tilde{\rho})$ and is not written out):

See equations (40)–(42) above.

$$
\begin{aligned}
J_3^{(3)}(p;\kappa;\tilde\rho) &= \frac{1}{\kappa Z_\kappa^2(2\pi)^2(1+\hat m_\kappa^2)^2}\left\{-1+\frac{\eta}{4}+\frac{\eta\hat m_\kappa^2}{4}+\bar p\left(\frac{3}{2}-\frac{\eta}{8}-\frac{7\eta\hat m_\kappa^2}{8}\right)-\frac{3\eta\bar p^2}{4}\right.\\
&+\frac{25\eta\bar p^3}{48}+\frac{1}{1+\hat m_\kappa^2}\left(\frac{4}{3}-\frac{4\eta}{15}-\bar p+\frac{\eta\bar p^2}{3}+\frac{\bar p^3}{12}-\frac{\eta\bar p^3}{6}+\frac{\eta\bar p^5}{120}\right)\\
&+\frac{1}{\bar p}\left[\left(1-\frac{\eta}{4}-(\bar p^2-\hat m_\kappa^2)\left(1-\frac{\eta}{2}+\frac{\eta}{4}(\bar p^2-\hat m_\kappa^2)\right)+\eta\hat m_\kappa^2\bar p^2\right)\frac{1}{2}\log\left(\frac{(\bar p+1)^2+\hat m_\kappa^2}{1+\hat m_\kappa^2}\right)\right.\\
&\left.\left.+\,2\hat m_\kappa\bar p\left(1-\frac{\eta}{2}+\frac{\eta}{2}(\bar p^2-\hat m_\kappa^2)\right)\left(\mathrm{Arctan}\left(\frac{\hat m_\kappa}{\bar p+1}\right)-\mathrm{Arctan}\,(\hat m_\kappa)\right)\right]\right\}\\
&= \frac{1}{\kappa Z_\kappa^2(2\pi)^2(1+\hat m_\kappa^2)^2}\left\{\frac{4}{3(1+\hat m_\kappa^2)}\left(1-\frac{\eta}{5}\right)-\frac{2}{3(1+\hat m_\kappa^2)^2}\bar p^2\right.\\
&\left.+\,\frac{2+\eta-2\hat m_\kappa^2+\eta\hat m_\kappa^2}{6(1+\hat m_\kappa^2)^3}\bar p^3-\frac{2(1+\eta-5\hat m_\kappa^2+\eta\hat m_\kappa^2)}{15(1+\hat m_\kappa^2)^4}\bar p^4+\mathcal{O}(\bar p^5)\right\}. \qquad (43)
\end{aligned}
$$

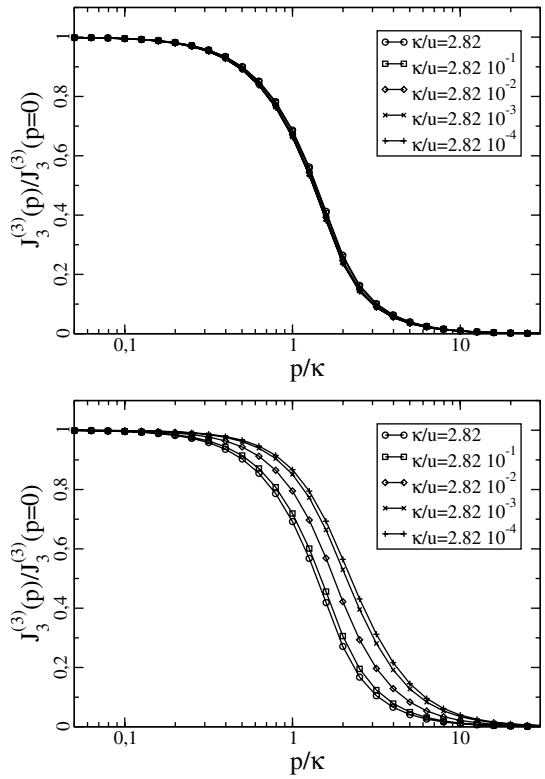

Fig. 9. The function $J_3^{(3)}(\kappa;p)/I_3^{(3)}(\kappa)$ for $\tilde\rho=0$ (top) and $\tilde\rho=6$ (bottom), as a function of (p/κ), for different values of κ/u.

d) $\bar p\le 2, m_\kappa^2\ge 0$.

See equation (43) above.

The function $J_3^{(3)}(p;\kappa;\rho)/J_3^{(3)}(p=0;\kappa;\rho)$ is displayed in Figure 9 for the two values $\tilde\rho=0$, and $\tilde\rho=6$. One sees that in both cases the p-dependence is concentrated in the region $p\sim\kappa$: $J_3^{(3)}(p;\kappa;\rho)$ is independent of p when $p\lesssim\kappa$, and it vanishes when $p\gtrsim\kappa$, a property that has been exploited in [19, 20]. For $\tilde\rho=0$, $J_3^{(3)}(\kappa;p)/J_3^{(3)}(\kappa;p=0)$ is essentially a function of p/κ only. For $\tilde\rho=6$ some residual dependence on κ remains.

Appendix C: Ultraviolet behavior of the self-energy

In this appendix we study the behavior of the self-energy $\Sigma(p)$ for $p\gg u$. We show that the solution of equation (16) reproduces the result of 2-loop perturbation theory, namely $\Sigma(p)=u^2/(96\pi^2)\log(p/u)$, albeit with a coefficient in front of the logarithmic that differs by 8%.

Consider first the exact flow equation for the 2-point function, equation (5), in vanishing external field (in this appendix $\rho=0$ throughout). At order 0-loop (indicated by the superscript [0]), this is simply:

$$\partial_\kappa\Gamma_\kappa^{(2)[0]}(p)=0. \qquad (44)$$

This equation has the solution

$$\Gamma_\kappa^{(2)[0]}(p)=p^2, \qquad (45)$$

where we used the initial condition at $\kappa=\Lambda$ that one deduces from equation (1), and adjusted the bare mass r to be at criticality ($\Sigma_{\kappa=0}(p=0;\rho=0)=0$, yielding $r^{[0]}=0$).

To go to 1-loop, one uses, in the r.h.s. of equation (5), the 0-loop expressions for both the propagator, $G_0(\kappa;p)=1/(p^2+R_\kappa(p))$, and the 4-point function $\Gamma_\kappa^{(4)[0]}(p_i)=u$. One gets

$$
\begin{aligned}
\partial_\kappa\Gamma_\kappa^{(2)[1]}(p) &= -\frac{u}{2}\int\frac{d^dq}{(2\pi)^d}\frac{\partial_\kappa R_\kappa(q)}{(q^2+R_\kappa(q))^2}\\
&= \frac{u}{2}\partial_\kappa\int\frac{d^dq}{(2\pi)^d}\frac{1}{q^2+R_\kappa(q)}\,.
\end{aligned} \qquad (46)
$$

The integration is immediate; by imposing criticality and the initial condition at $\kappa=\Lambda$, one obtains

$$\Gamma_\kappa^{(2)[1]}(p)-p^2=\frac{u}{2}\int\frac{d^dq}{(2\pi)^d}\left\{\frac{1}{q^2+R_\kappa(q)}-\frac{1}{q^2}\right\}, \qquad (47)$$

which is in fact independent of the momentum p.

The 1-loop expression for the 4-point function, which will be needed shortly, is obtained similarly:

$$\partial_\kappa \Gamma_\kappa^{(4)[1]}(p,-p,l,-l) = u^2 \int \frac{d^dq}{(2\pi)^d} \partial_\kappa R_\kappa(q) G_0^2(\kappa;q) \times \{G_0(\kappa;q) + G_0(\kappa;p+l+q) + G_0(\kappa;p-l+q)\}, \tag{48}$$

which can be integrated easily to give

$$\Gamma_\kappa^{(4)[1]}(p,-p,l,-l) = u\frac{u^2}{2} \int \frac{d^dq}{(2\pi)^d} G_0(\kappa;q) \times \{G_0(\kappa;q) + G_0(\kappa;p+l+q) + G_0(\kappa;p-l+q)\}, \tag{49}$$

where we imposed the initial condition

$$\Gamma_{\kappa=\Lambda}^{(4)}(p,-p,l,-l,\rho=0) = u$$

(the integrand in Eq. (49) should, for finite Λ, be subtracted from its value at $\kappa = \Lambda$ in order to satisfy this initial condition; the corresponding contribution, however, vanishes in the limit $\Lambda \to \infty$, and we assume here that Λ is large enough so that it can be neglected.)

Going now to 2-loop, one puts in the r.h.s. of equation (5) the 1-loop expressions of both the propagator and the 4-point functions. Since we are interested only in the momentum dependence of the 2-point function, we consider only the terms in the flow equation that depend on p, i.e., $\Sigma_\kappa(p) = \Gamma_\kappa^{(2)}(p) - \Gamma_\kappa^{(2)}(0) - p^2$. Since the momentum dependent terms originate entirely from the contribution of order u^2 in $\Gamma^{(4)[1]}$, we can use G_0 as propagator. We have therefore

$$\partial_\kappa \Sigma_\kappa^{[2]}(p) = \frac{u^2}{2} \int \frac{d^dl}{(2\pi)^d} \partial_\kappa R_\kappa(l) G_0^2(\kappa;l) \times \int \frac{d^dq}{(2\pi)^d} G_0(\kappa;q)(G_0(\kappa;p+l+q) - G_0(\kappa;l+q)). \tag{50}$$

This expression can also be integrated to give

$$\Sigma_\kappa^{[2]}(p) = -\frac{u^2}{6} \int \frac{d^dl}{(2\pi)^d} \int \frac{d^dq}{(2\pi)^d} G_0(\kappa;l) G_0(\kappa;q) \times (G_0(\kappa;p+l+q) - G_0(\kappa;l+q)). \tag{51}$$

At this point, we need to deal with the fact that the 2-loop expression for the self-energy is IR divergent. And indeed when $\kappa \to 0$ at fixed p, the integral in equation (51) diverges. In order to go around this difficulty, we consider the derivative $\partial_p \Delta\Gamma_\kappa^{(2)}(p)$

$$\frac{\partial \Sigma_\kappa^{[2]}(p)}{\partial |p|} = \frac{u^2}{3} \int \frac{d^dl}{(2\pi)^d} \int \frac{d^dq}{(2\pi)^d} G_0(l) G_0(q) \times G_0^2\,(p+l+q)(\mathbf{l}+\mathbf{q}+\mathbf{p}).\hat{\mathbf{p}}\,(1 + R'_\kappa(l+p+q)), \tag{52}$$

where $\hat{\mathbf{p}} \equiv \mathbf{p}/|\mathbf{p}|$ and $R'_\kappa(q) \equiv \partial_{q^2} R_\kappa(q)$. The limit $\kappa \to 0$ can now be taken, and yields

$$\frac{\partial \Sigma_{\kappa=0}^{[2]}(p)}{\partial |p|} = \frac{u^2}{6} \int \frac{d^dq}{(2\pi)^d} \frac{2q.\hat{p}}{q^4} \int \frac{d^dl}{(2\pi)^d} \frac{1}{l^2} \frac{1}{(l+p-q)^2}. \tag{53}$$

Performing the integral over l and those over $\cos\theta = \hat{\mathbf{p}}.\hat{\mathbf{q}}$ and $|\mathbf{q}|$, one recovers the well known result (in $d = 3$):

$$\begin{aligned} \frac{\partial \Sigma_{\kappa=0}^{[2]}(p)}{\partial |p|} &= \frac{1}{24} \frac{u^2}{(2\pi)2} \int_0^\infty \frac{d|q|}{|q|} \times \int_0^\pi d\theta \frac{\sin\theta\, \cos\theta}{(p^2+q^2-2|p||q|\cos\theta)^{1/2}} \\ &= \frac{u^2}{96\pi^2} \frac{1}{|p|}. \end{aligned} \tag{54}$$

Let us now turn to the perturbative limit of equation (16). Note that, at both 0- and 1-loop orders, the predictions of equations (5) and (16) for the self-energy coincide. A difference arises at 2-loop order since, at the LO of the approximation scheme, we should insert in equation (50) $\Gamma_\kappa^{(4)[1]}(p,-p,0,0)$ instead of $\Gamma_\kappa^{(4)[1]}(p,-p,l,-l)$ as we did in the exact calculation, where the expression of $\Gamma^{(4)[1]}$ is given in equation (49). That is, the LO flow equation reads

$$\partial_\kappa \Sigma_\kappa^{[2]LO}(p) = \frac{u^2}{2} \int \frac{d^dl}{(2\pi)^d} \partial_\kappa R_\kappa(l) G_0^2(\kappa;l) \times \int \frac{d^dq}{(2\pi)^d} G_0(\kappa;q)(G_0(\kappa;p+q) - G_0(\kappa;q)). \tag{55}$$

In contrast to what happens with equation (50), here the integration over κ can no longer be done analytically and we have to deal with a third integral. Let us call κ' the variable of this integration, and integrate over $t' = \log(\kappa'/|p|)$. After making the changes of variables $q \to |p|q$ and $l \to |p|l$, one obtains:

$$\begin{aligned} \Sigma_\kappa^{(2)[2]LO}(p) &= -\frac{u^2}{2} |p|^{2(d-3)} \\ &\times \int_{\log\kappa/|p|}^\infty dt \int \frac{d^dl}{(2\pi)^d} \partial_{t'} R_{\kappa'}(l) G_0^2(\kappa;l) \\ &\times \int \frac{d^dq}{(2\pi)^d} G_0(\kappa;q)(G_0(\kappa;\hat{p}+q) - G_0(\kappa;q)). \end{aligned} \tag{56}$$

Now, the derivative with respect to $|p|$ is very simple because, in $d = 3$, it only enters in the integration limit. One has:

$$\frac{\partial \Sigma_{12}^{(2)[2]LO}(p)}{\partial |p|} = -\frac{u^2}{2|p|} \int \frac{d^3l}{(2\pi)^3} \partial_t R_\kappa(l) G_0^2(\kappa;l) \times \int \frac{d^3q}{(2\pi)^3} G_0(\kappa;q)(G_0(\kappa;\hat{p}+q) - G_0(q)), \tag{57}$$

where $t = \log(\kappa/|p|)$. In can be verified that the first term, i.e., that containing $\hat{p}$, vanishes when $\kappa \ll |p|$. In this limit:

$$\frac{\partial \Sigma_{\kappa=0}^{[2]\,LO}(p)}{\partial |p|} = \frac{1}{2}\frac{u^2}{|p|}\int \frac{d^3l}{(2\pi)^3}\partial_t R_\kappa(l) G_0^2(\kappa; l) \times \int \frac{d^3q}{(2\pi)^3} G_0^2(\kappa; q) = \frac{u^2}{9\pi^4}\frac{1}{|p|}. \quad (58)$$

Comparing equations (54) and (58) one sees that they both predict a logarithmic behavior for the self-energy, the ratio of their respective coefficients being:

$$\frac{1/(9\pi^4)}{1/(96\pi^2)} \simeq 1.08. \quad (59)$$

References

1. C. Wetterich, Phys. Lett. B **301**, 90 (1993)
2. U. Ellwanger, Z. Phys. C **58**, 619 (1993)
3. N. Tetradis, C. Wetterich, Nucl. Phys. B **422**, 541 (1994)
4. T.R. Morris, Int. J. Mod. Phys. A **9**, 2411 (1994)
5. T.R. Morris, Phys. Lett. B **329**, 241 (1994)
6. C. Bagnuls, C. Bervillier, Phys. Rep. **348**, 91 (2001)
7. J. Berges, N. Tetradis, C. Wetterich, Phys. Rep. **363**, 223 (2002)
8. U. Ellwanger, Z. Phys. C **62**, 503 (1994); U. Ellwanger, C. Wetterich, Nucl. Phys. B **423**, 137 (1994); T.R. Morris, Phys. Lett. B **334**, 355 (1994); U. Ellwanger, M. Hirsch, A. Weber, Eur. Phys. J. C **1**, 563 (1998); J.M. Pawlowski, D.F. Litim, S. Nedelko, L. von Smekal, Phys. Rev. Lett. **93**, 152002 (2004); J. Kato, e-print `arXiv:hep-th/0401068`; C.S. Fischer, H. Gies, JHEP **0410**, 048 (2004)
9. S. Weinberg, Phys. Rev. D **8**, 3497 (1973)
10. G.R. Golner, Exact renormalization group flow equations for free energies and N-point functions in uniform external fields, e-print `arXiv:hep-th/9801124`.
11. A. Parola, L. Reatto, Adv. Phys. **44**, 211 (1995); A. Parola, L. Reatto, D. Pini, Phys. Rev. E. **48**, 3321 (1993)
12. L. Canet, B. Delamotte, D. Mouhanna, J. Vidal, Phys. Rev. B **68** 064421 (2003)
13. B. Delamotte, D. Mouhanna, M. Tissier, Phys. Rev. B **69**, 134413 (2004); L. Canet, B. Delamotte, e-print `arXiv:cond-matt/0412205`
14. J.P. Blaizot, R. Mendez Galain, N. Wschebor, Phys. Lett. B **632**, 571 (2006)
15. D.F. Litim, JHEP **0111**, 059 (2001), e-print `arXiv:hep-th/0111159`
16. G. Von Gersdorff, C. Wetterich, Phys. Rev. B **64**, 054513 (2001), e-print `arXiv:hep-th/0008114`
17. H. Ballhausen, J. Berges, C. Wetterich, Phys. Lett. B **582**, 144 (2004), e-print `arXiv:hep-th/0310213`
18. C. Bervillier, e-print `arXiv:hep-th/0501087`
19. J.P. Blaizot, R. Mendez-Galain, N. Wschebor, Phys. Rev. E **74**, 051116 (2006), e-print `arXiv:hep-th/0512317`
20. J.P. Blaizot, R. Mendez-Galain, N. Wschebor, Phys. Rev. E **74**, 051117 (2006), e-print `arXiv:hep-th/0603163`
21. R.D. Ball, P.E. Haagensen, J.I. Latorre, E. Moreno, Phys. Lett. B **347**, 80 (1995)
22. J. Comellas, Nucl. Phys. B **509**, 662 (1998)
23. D. Litim, Phys. Lett. B **486**, 92 (2000); D. Litim, Phys. Rev. D **64**, 105007 (2001); D. Litim, Nucl. Phys. B **631**, 128 (2002); D. Litim, Int. J. Mod. Phys. A **16**, 2081 (2001)
24. L. Canet, B. Delamotte, D. Mouhanna, J. Vidal. Phys. Rev. D **67**, 065004 (2003)
25. J.P. Blaizot, R. Mendez Galain, N. Wschebor, Europhys. Lett. **72 (5)**, 705 (2005)
26. J. Berges, N. Tetradis, C. Wetterich, Phys. Rev. Lett. **77**, 873 (1996)
27. N. Tetradis, D.F. Litim, Nucl. Phys. B **464**, 492 (1996)
28. R. Guida, J. Zinn-Justin, J. Phys. A **31**, 8103 (1998)
29. G. Baym, J.-P. Blaizot, M. Holzmann, F. Laloë, D. Vautherin, Phys. Rev. Lett. **83**, 1703 (1999)
30. X. Sun, Phys. Rev. E **67**, 066702 (2003)
31. B.M. Kastening, Phys. Rev. A **69**, 043613 (2004)